ACCEPTED MANUSCRIPT

Authors: Adam Frączyk, Krzysztof Kuś, Adam Wojtkowiak

A STUDY OF NON-ISOTHERMAL PRIMARY CRYSTALLIZATION KINETICS OF Fe$_{95}$Si$_5$ AMORPHOUS ALLOY

Adam Frączyk[*], *Krzysztof Kuś, Adam Wojtkowiak*

Departament of Materials and Machine Technology
University of Warmia and Mazury in Olsztyn

K e y w o r d s: metallic glass, energy activation, Avrami exponent, crystallization kinetics parameter, DSC

Abstract

The paper discusses the primary crystallization process of metallic Fe95Si5 glass, which was studied by differential scanning calorimetry (DSC) with non-isothermal methods. The activation energy of the crystal transformation was calculated in accordance with the equations developed by Kissinger, Mahadevan and the modified equation of Augis and Benntt. Depending on the method used, this energy varies within the range $Ea = 242.0 - 254.2$ kJ / mol. The exponent of crystallization kinetics of the amorphous phase n was subsequently determined and proven to vary within the range of $n = 2.40 - 2.52$, depending on the method applied in order to calculate the transformation activation energy.

Introduction

The excellent soft magnetic properties of amorphous alloys have been used in many fields of industrial and new metallic glasses and their properties are still under investigation (LI et al. 2008, SAHINGOZA et al. 2004, NOBUYUKI et al. 2007).

It was established that thermal treatment of metallic glasses and the nanocrystallization process improve their properties. The possibility to control the crystallization process of amorphous alloys is particularly important in order to obtain specific structures of materials. Therefore, it is essential to properly understand crystallization kinetics of metallic glasses.

The crystallization kinetics in chalcogenide glasses can be investigated using isothermal and non-isothermal methods, and the results can be interpreted in terms of several theoretical models e. g. (KISSINGER 1957, OZAWA 1970, MATUSITA et al. 1979, MATUSITA et

---

[*] Corespondence: Departament of Materials and Machine Technology University of Warmia and Mazury in Olsztyn, Poland, Oczapowskiego str. 11, 10-719 Olsztyn, phone: +48 89 523 44 43, e-mail: adam.fraczyk@uwm.edu.pl

al. 1980, KONG et al. 2011, REZAEI-SHAHREZA et al. 2017). Recently, many authors have also been using new isoconversional methods for determining the crystallization parameters of amorphous alloys during non-isothermal heating (REZAEI-SHAHREZA et al. 2017, ANSARINIYA et al. 2018, JAAFARI et al. 2018).

Isothermal analysis is based on JMA equation, which constitutes a primary method for determining crystallization parameters. However, many authors apply non-isothermal techniques, which allow them to perform experiments. Different values of the crystallization kinetic parameters are observed in various Fe-based amorphous alloys, for example the Avrami exponent estimated values range from 1.0 to 4.0 (GIBSON et al. 1987, SANTOS et al. 2002.). Moreover, the activation energy for the same alloy can be calculated based on different models and equations. The purpose of the research is to determine the value of the activation energy of the primary crystallization process based on the equations of Kissinger, Mahadevan and the modified equation of Augis and Benntt. Also, the exponent of crystallization kinetics (Avrami exponent) n, which reflects the mechanism of crystalline phase formation, was determined in the paper.

Theory

In the study of the kinetics of crystallization of amorphous alloys, two parameters are most often determined - activation energy E_a and exponent of crystallization kinetics (Avrami exponent) n.

In calorimetric measurements, isothermal and non-isothermal methods can be used. Most methods is based on Johnson-Mehl-Avrami-Kolmogorov (JMAK) equation of isothermal transformation kinetics (MÁLEK 2000, WANG et al. 2014):

$$x(t) = 1 - \exp\left(-Kt^n\right) \qquad (1)$$

where: $x(t)$ is volume fraction transformed after time t, n is Avrami kinetics exponent (the exponent which reflects the nucleation rate and the growth morphology), K is the reaction rate constant. The temperature dependence is usually assigned from Arrhenius equation:

$$K = K_0 \exp\left(\frac{-E_a}{RT}\right) \qquad (2)$$

where: E_a is the activation energy for the crystallization reaction, K_0 is the frequency factor and R is the gas constant.

The non-isothermal crystallization is characterized by a constant heating rate. The relation between the sample temperature T and the heating rate β can be determined as:

$$T=T_0+ \beta t \tag{3}$$

Among others, there are models developed by Kissinger (KISSINGER 1957), Ozawa (OZAWA 1970), Mahadevan (MAHADEVAN et al. 1986) and Augis-Benntt (AUGIS et al. 1978,).
These methods are based on JMAK theory (Eq.1) and the logarithmic form of equation 2. These models consider that at the top of crystallization peak DSC the amount of crystallized fraction is $x_p=0,63$. Using the highest rate of a transformation at maximum peak approximations interpreted in this equations, respectively :

a) Kissinger model

$$\ln\left(\frac{\beta}{T_p^2}\right)=\frac{-E_a}{RT_p} + \ln\left(\frac{K_0 R}{E_a}\right) \tag{4}$$

b) Mahadevan et al. model

$$\ln(\beta)=\frac{-E_a}{RT_p} + \ln\left(\frac{K_0 E_a}{R}\right) \tag{5}$$

c) A modified form of the Augis and Bennt model

$$\ln\left(\frac{\beta}{T_p}\right)=\frac{-E_a}{RT_p} + \ln(K_0) \tag{6}$$

where: T_p peak of the temperature, $\beta=dT/dt$ heating rate.

The partial $ln(K_0R/E_A)$, $ln(K_0E_A/R)$ and $ln(K_0)$ in equations 4, 5 and 6 are constant. From the slope and the intercept of the straight line (Eq.4,5,6) it is possible to derive the value of the activation energy E_a and the pre-exponential factor K_0 of the crystallization process, respectively.

Avrami's exponent n is the second very important crystallization parameter. There are also various methods of determining its value. In the model developed by Ozawa, time in Eq. (1) was replaced by temperature with Eq. (3). Thus, the following equation was obtained:

$$x(t) = 1 - \exp\left[-\left\{\frac{K(T-T_0)}{\beta}\right\}\right] \qquad (7)$$

After transformations and double logarithms, Eq. (7) takes the following form:

$$\ln\left[-\ln(1-x)\right] = -n\ln(\beta) + n\ln(T-T_0) \qquad (8)$$

After drawing the plot $ln[-ln (1 - x)]$ versus $ln(\beta)$ from various DSC thermograms, we can derive the value of the Avrami exponent n from the slope of the straight line (Eq.8).

We can also determine the Avrami exponent n from the equation presented by the authors (GAO et al.1986, JAKUBCZYK et al. 2008):

$$n = \left(\frac{dx}{dt}\right)_p RT_p^2 (0{,}37\,\beta E_a)^{-1} \qquad (9)$$

Where: $(dx/dt)_p$ – The maximum crystallization rate.

Experimental

The amorphous samples – Fig.1 were obtained by rapid solidification from the melt using the melt-spinning method. The obtained ribbon was 20 mm wide and and 0,03 mm thick, with nominal composition of $Fe_{95}Si_5$ – Fig.2.

The crystallization process was investigated by differential scanning calorimetry (DSC) in nitrogen atmosphere using a NETZSCH DSC 204 instrument. Temperature and energy calibrations of the instrument were performed using the well-known melting temperatures and melting enthalpies of high-purity zinc and indium supplied with the instrument. The sample masses used for DSC measurements were about several milligrams. The samples were heated from 340 K to 840 K using different rates β= 5, 10, 20 and 30 K min^{-1} respectively.

Results and discussion

DSC thermograms for the crystallization process of the $Fe_{95}Si_5$ at various heating rates are shown in Fig. 3. The two crystallization peaks of $Fe_{95}Si_5$ involve two resolved phase transformation. When the heating rate increases, the position of both peaks was shifted to the higher temperatures. It was proven (FRĄCZYK 2011) that the first peak corresponds to the phase formation α-Fe(Si). The observed shift of the onset of crystallization T_x and to higher temperatures is the result of the induction time of the nucleation process. There is a nucleation time during crystallization. When the heating rate increases, the onset of crystallization shifts to higher temperatures.

The activation energy E_a of primary crystallization of metallic glass $Fe_{95}Si_5$ was calculated by Kissinger, Mahadevan and through a modified form of the Augis and Benntt model (4-6). For this purpose, the graphs $ln(\beta/T_p^2)$ vs. $10^3/T_p$ (Fig.4), $ln(\beta)$ vs. $10^3/T_p$ (Fig.5) and $ln(\beta/T_p^2)$ vs. $10^3/T_p$ (Fig.6) are plotted respectively for the amorphous alloy. From the slope $(-E_a/R)$ of the line activation energy E_a of an amorphous alloy can be obtained. A best fit for the results was calculated by the least-square method. The arithmetic mean as well as the standard deviation were calculated for the activation energies. The results are presented in Table 1.

The crystallized fraction x at any temperature T is given as $x(T) = Ax(T)/A$, where A and Ax are the total and partial (at generic temperature T) areas of exothermic peak, respectively. Fig.7 shows the relationship between the crystallized volume fraction and time of the first exothermic peak of amorphous $Fe_{95}Si_5$ alloy. After differentiating the data from Fig. 5 as a function of time t, we can show the dependence of the crystallization rate dx/dt versus temperature T – Fig.8.

The Avrami exponent n was calculated by substituting the maximum value of dx/dt into Eq.9 for different heating rates. The primary crystallization parameters are presented in Table 1.

The activation energy E_a and Avrami exponent n is one of the two most important kinetic parameters describing the crystallization of an amorphous alloy. The highest activation energy E_a was obtained based on the Mahadevan equation 5, whereas the lowest value of this energy was obtained by the Kissinger equation 4. The difference in extreme values of E_a amounts to almost 5%.

The author (AL-HENITI 2009) obtained similar results when he studied the crystallization kinetics of $Fe_{78}Ni_{1.5}Si_9B1_3$ metallic glasses.

Conclusions

The estimated values of activation energies and Avrami exponent *n,* connected with the first peak temperature in the continuous heating DSC curves of the amorphous $Fe_{95}Si_5$ alloy were calculated by the means of acclaimed methods.

The values of Avrami exponent *n* indicate that during the first stages of the crystallization process a crystal growth controlled respectively by diffusion and by interface takes place.

In order compare the activation energy of different amorphous alloys the same equation or model should be applied.

References

AL-HENITI S.H. 2009. Kinetic study of non-isothermal crystallization in $Fe_{78}Si_9B_{13}$ metallic glass. Journal of Alloys and Compounds 484, p. 177–184.

ANSARINIYA M., SEIFODDINI A., HASANI S. 2018. $(Fe_{0.9}Ni_{0.1})_{77}Mo_5P_9C_{7.5}B_{1.5}$ bulk metallic glass matrix composite produced by partial crystallization: The non-isothermal kinetic analysis. Journal of Alloys and Compounds 763 p. 606 – 612.

AUGIS J.A., BENNTT J.E. 1978, J. Therm. Anal. 13, 283.

FRĄCZYK A. 2011. The activation energy of primary crystallization of $Fe_{95}Si_5$ metallic glass. Technical Science., 14(1), 93-100.

GAO Y.Q., WANG W. 1986. On the activation energy of crystallization in metallic glasses, J. Non-Cryst. Solids, 81,129 –134.

GIBSON M.A., DELAMORE G.W. 1987. J. Mater. Sci. 22, 4550.

JAKUBCZYK E., KRAJCZYK A., JAKUBCZYK M. 2008. Crystallization of amorphous $Fe_{78}Si_9 B_{13}$ alloy. Journal of Physics: Conference Series 79 (2007) 012008

JUNG H. Y., STOICA M., YI S., KIM D. H., ECKERT J. 2015. Crystallization Kinetics of $Fe_{76.5-x} C_{6.0}Si_{3.3}B_{5.5}P_{8.7}Cu_x$, (x = 0, 0.5, and 1 at. pct) Bulk Amorphous Alloy. Metallurgical and Materials Transactions, Vol. 46A, p. 2415-2421.

JAAFARI Z., SEIFODDINI A. , HASANI S., REZAEI-SHAHREZA P. 2018. Kinetic analysis of crystallization process in $[(Fe_{0.9}Ni_{0.1})_{77} Mo_5P_9C_{7.5}B_{1.5}]_{100-x}Cu_x(x = 0.1$ at.%) BMG. Journal of Thermal Analysis and Calorimetry 134, p. 1565–1574.

KISSINGER H. E. 1957. Reaction kinetics in differential thermal analysis. Analytical Chemistry 29, p.1702-1706.

KONG L.H., GAO Y.L., SONG T.T., WANG G., ZHAI Q. J. 2011. Non-isothermal crystallization kinetics of FeZrB amorphous alloy. Thermochimica Acta 522, p.166–172.

LI H.X., JUNG H.Y., YI S. 2008. Glass forming ability and magnetic properties of bulk metallic glasses $Fe_{68.7-x}C_{7.0}Si_{3.3}B_{5.5}P_{8.7}Cr_{2.3}Mo_{2.5}Al_{2.0}Co_x$ (x = 0–10). Journal of Magnetism and Magnetic Materials, Vol. 320, p.241-245.

MAHADEVAN S., GIRIDHAR A., SINGH A.K. 1986. J. Non-Cryst. Solids 88, 11.

MÁLEK J. 2000. Kinetic analysis of crystallization processes in amorphous materials. Thermochimica Acta Vol. 355, p. 239-253.

MATUSITA K, SAKKA S. 1979. PHYS. CHEM. GLASSES 20, 77.

MATUSITA K, SAKKA S. 1980. J. NON-CRYST. SOLIDS 38&39, 741

NOBUYUKI N., KENJI A., AKIHISA I. 2007. Novel applications of bulk metallic glass for industrial products. Journal of Non-Crystalline Solids, Vol. 353, p. 3615-3621

OZAWA T. 1970. Kinetic analysis of derivative curves in thermal analysis. Journal of Thermal Analysis 2, p.301-324.

REZAEI-SHAHREZA P., SEIFODDINI A., HASANI S. 2017. Thermal stability and crystallization process in a Fe-based bulk amorphous alloy: The kinetic analysis. Journal of Non-Crystalline Solids 471, p. 286–294.

REZAEI-SHAHREZA P., SEIFODDINI A., HASANI S. 2017. Non-isothermal kinetic analysis of nano-crystallization process in $(Fe_{41}Co_7Cr_{15}Mo_{14}Y_2C_{15})_{94}B_6$ amorphous alloy. Thermochimica Acta 652, p. 119–125.

SAHINGOZA R., EROLA M., GIBBS M. R.J. 2004.Observation of changing of magnetic properties and microstructure of metallic glass $Fe_{78}Si_9B_{13}$ with annealing. Journal of Magnetism and Magnetic Materials, Vol. 271, p. 74-78.

SANTOS D.S., SANTOS D.R., BIASIC R.S. 2002. J. Magn. Magn. Mater. 242–245, 882.

WANG T., YANG X., LI Q. 2014. Effect of Cu and Nb additions on crystallization kinetics of $Fe_{80}P_{13}C_7$ bulk metallic glasses. Thermochimica Acta 579 p. 9–14.

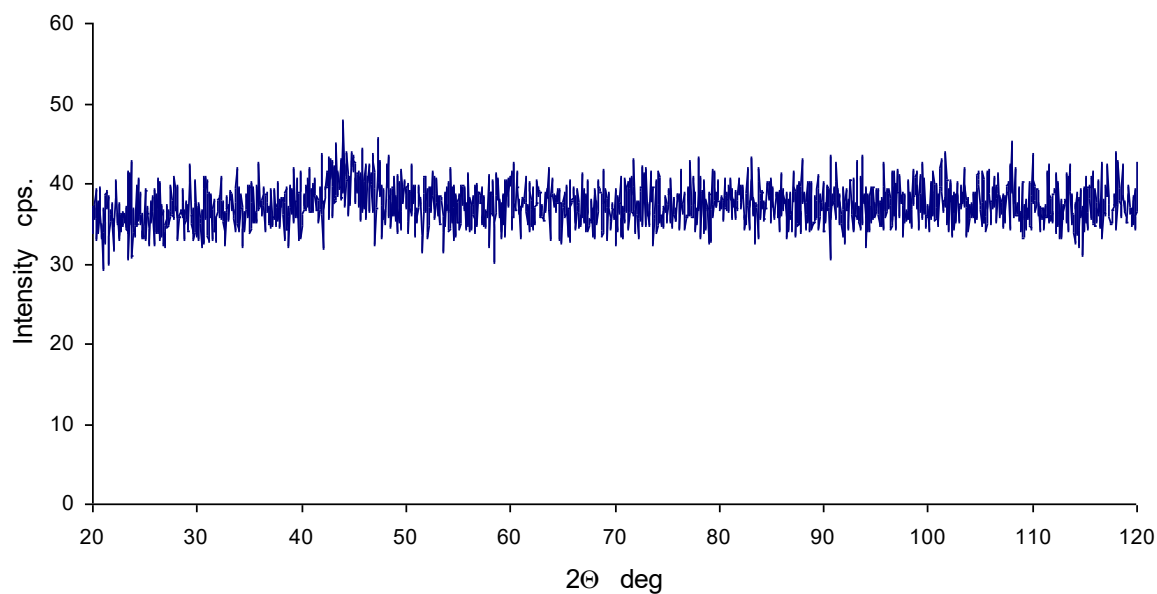Fig.1. XRD pattern for the $Fe_{95}Si_5$ amorphous alloy.

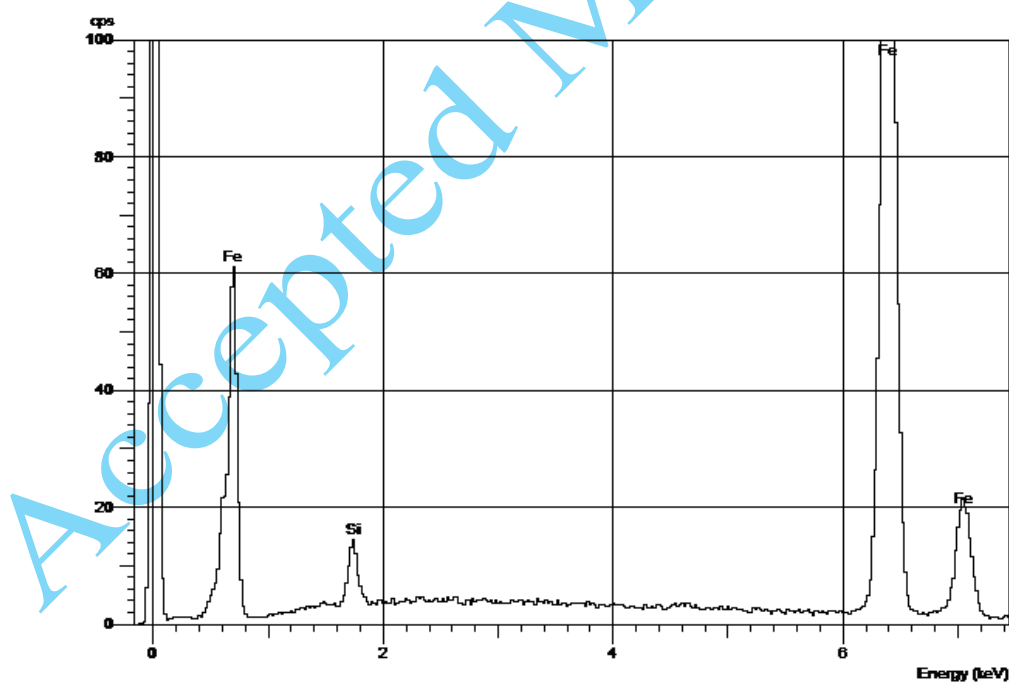Fig.2. EDS Spectrum for $Fe_{95}Si_5$ amorphous alloy.
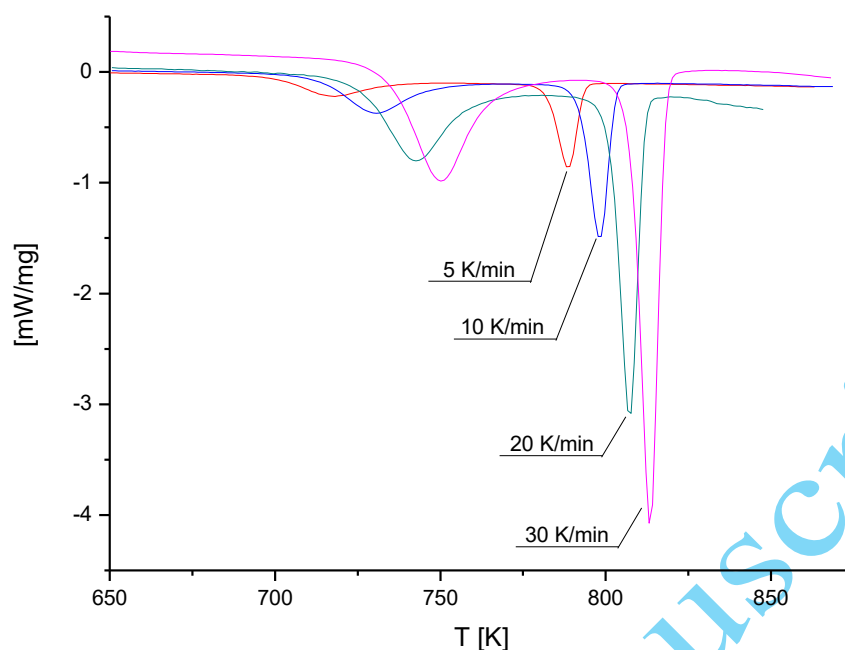
Fig.3. DSC curves of Fe$_{95}$Si$_5$ for several heating rates showing the primary crystallization process (first peak) and secondary crystallization (second peak).

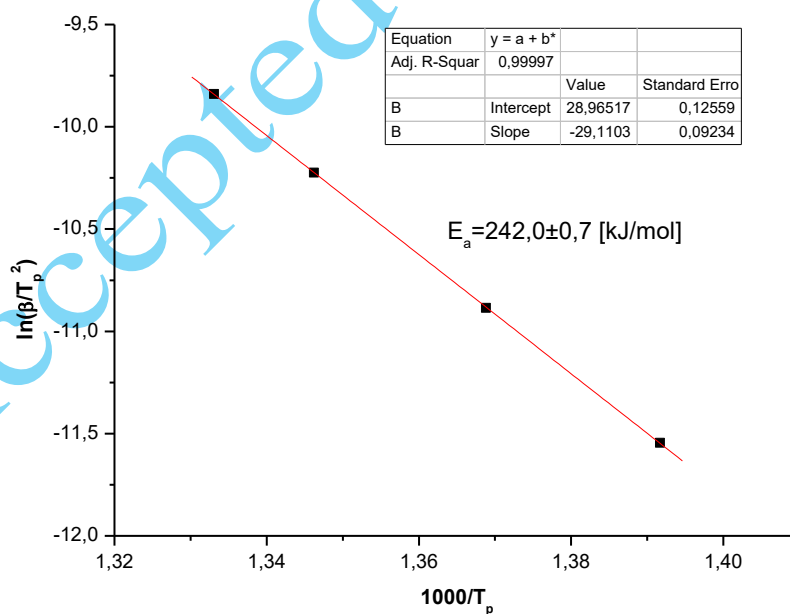| Equation	y = a + b*		
Adj. R-Squar	0,99997		
		Value	Standard Erro
B	Intercept	28,96517	0,12559
B	Slope	-29,1103	0,09234

E_a=242,0±0,7 [kJ/mol]

Fig.4. ln(β/T_p^2) versus 1000/Tp plot for determination of the activation energy E_a from a set of DSC scans with different heating rates (5, 10, 20 and 30 K/min). The analysis was performed for the first of the observed exothermic reaction DSC amorphous alloy Fe$_{95}$Si$_5$.

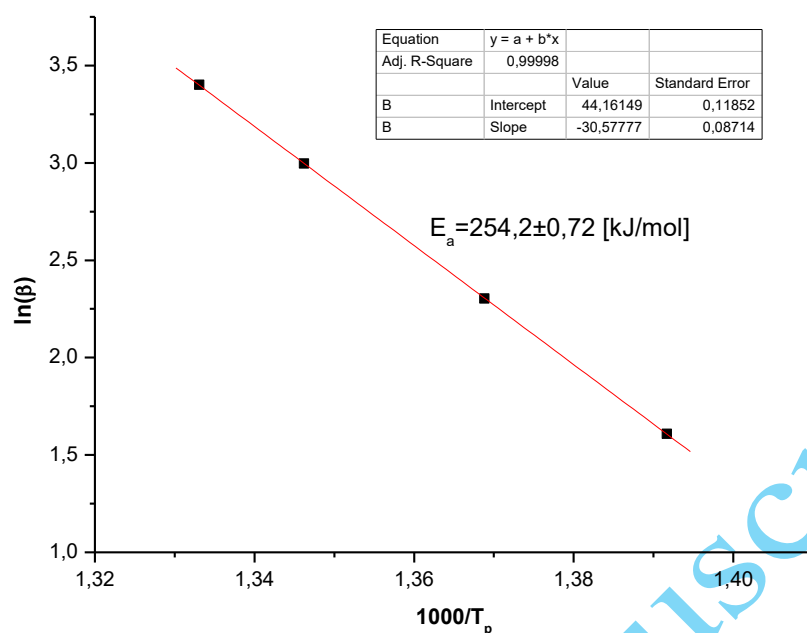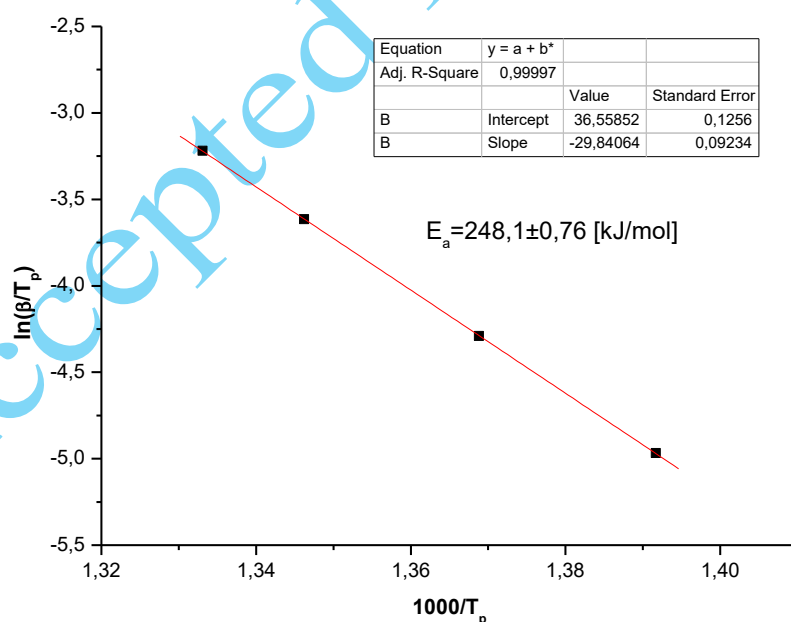| Equation	y = a + b*x		
Adj. R-Square	0,99998		
		Value	Standard Error
B	Intercept	44,16149	0,11852
B	Slope	-30,57777	0,08714

$E_a = 254,2 \pm 0,72$ [kJ/mol]

Fig.5. $\ln(\beta)$ versus $1000/T_p$ plot for determination of the activation energy E_a from a set of DSC scans with different heating rates (5, 10, 20 and 30 K/min). The analysis was performed for the first of the observed exothermic reaction DSC amorphous alloy $Fe_{95}Si_5$.

Equation	y = a + b*		
Adj. R-Square	0,99997		
		Value	Standard Error
B	Intercept	36,55852	0,1256
B	Slope	-29,84064	0,09234

$E_a = 248,1 \pm 0,76$ [kJ/mol]

Fig.6. $\ln(\beta/T_p)$ versus $1000/T_p$ plot for determination of the activation energy E_a from a set of DSC scans with different heating rates (5, 10, 20 and 30 K/min). The analysis was performed for the first of the observed exothermic reaction DSC amorphous alloy $Fe_{95}Si_5$.
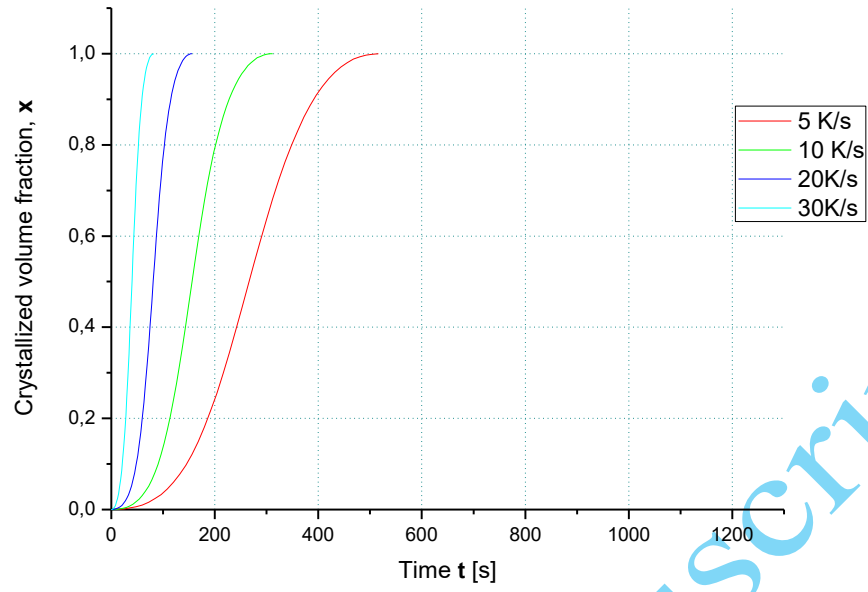
Fig. 7. Crystallized volume fraction x as a function of time t for $Fe_{95}Si_5$ metallic glass at different heating rates β.

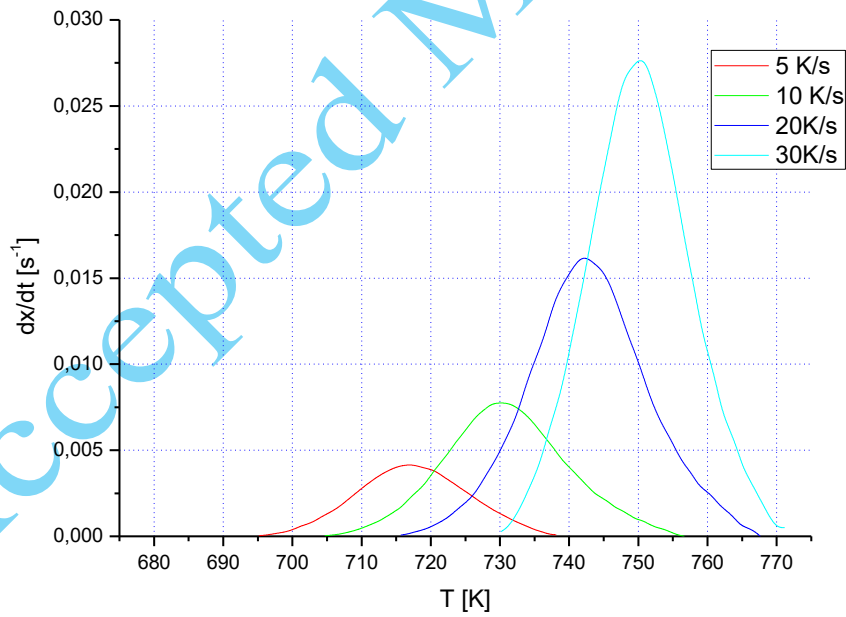Fig.8. Curves crystallization rate dx/dt versus temperature T for $Fe_{95}Si_5$ amorphous alloy at different heating rates β.

Table 1.

Parameters of primary crystallization kinetics of $Fe_{95}Si_5$ metallic glass.

Parameter	by Kissinger equation	by Mahadevan et al. equation	by modified form Augis & Benntt equation
Ea [kJ/mol]	242,0	254,2	248,1
n	2,52	2,46	2,40